Division of Cardiology, Nanjing First Hospital, Nanjing Medical University, Nanjing, China

Cardamonin protects against adverse cardiac remodeling through mTORC1 inhibition in mice with myocardial infarction

Wei You, Zhiming Wu, Fei Ye*, Xiangqi Wu*

Received June 20, 2018, accepted July 26, 2018

**Corresponding authors: Xiangqi Wu; Fei Ye, Division of Cardiology, Nanjing First Hospital, Nanjing Medical University, 68 Changle Rd, 210006 Nanjing, China.*
wuxiangqi2018@sina.com

Pharmazie 73: 508-512 (2018) *doi: 10.1691/ph.2018.8600*

The mTORC1-dependent signaling pathway is mainly involved in the adverse left ventricular remodeling (ALVR) process after myocardial infarction (MI). However, whether mTORC1 inhibition by cardamonin attenuates ALVR after MI is still not reported. Twenty mice were randomly assigned into three groups: sham group (10 ml/kg/day PBS, n=6), model group (MI and 10 ml/kg/day PBS, n=7) and cardamonin-treated group (MI and 20 mg/kg/day cardamonin, n=7). All groups received an intraperitoneal injection accordingly for two weeks. Heart and body mass were measured. Cardiac function was assessed by echocardiography. The collagen deposition, area of cardiomyocytes and cell apoptosis of border area were evaluated using Masson's staining, WGA staining and TUNEL assay, respectively. The 4E-binding protein 1 (4E-BP1) and ribosomal S6 (S6) in myocardium were determined by western blot. mTOR-Raptor association was tested by co-immunoprecipitation assay in H9C2 cell line. Treatment with cardamonin, MI mice displayed that heart hypertrophy and heart dysfunction were alleviated, and cardiac fibrosis, cardiomyocyte size and cell apoptosis of border area were decreased ($P<0.05$). Besides, cardamonin can inhibit 4E-BP1 and S6 phosphorylation in heart of MI mice and H9C2 cell line ($P<0.05$). Furthermore, cardamonin disrupted mTOR-Raptor association in vitro. Cardamonin exerted cardio-protection against ALVR through mTORC1 inhibition.

1. Introduction

Myocardial infarction (MI) is the common presentation of cardiovascular diseases and is one of leading causes of morbidity and mortality (Benjamin et al. 2017). MI occurs when a major coronary artery is blocked by a thrombus due to plaque rupture, which leads to localized cardiomyocytes death because of the lack of sufficient oxygenation and nutrition (Zaman et al. 2000). Following MI, the left ventricle (LV) undergoes molecular, cellular and extracellular matrix alterations which notably affect myocardial size, shape and function. Adverse left ventricular remodeling (ALVR) after MI due to necrosis, inflammation, cardiomyocyte hypertrophy and excessive fibrosis can eventually results in heart failure (HF) (Cohn et al. 2000). Despite the widespread use of traditional drug medication such as angiotensin-converting enzyme inhibitors and beta-blockers, the incidence of end-stage heart failure still remains high. Thus, elucidating the mechanisms underlying ALVR after MI may yield novel therapeutic targets for the treatment of HF patients is essential.

In recent years, protein synthesis involved in the ALVR process received remarkable attention (Buss et al. 2009). One important molecule of protein synthesis is the mechanistic target of rapamycin (TOR) complex 1 or mammalian target of TOR complex 1 (mTORC1) involved in cell proliferation, growth, and differentiation (Laplante et al. 2012). mTOR is mainly activated *via* the protein kinase B (Akt)/ phosphatidylinositol 3-kinase (PI3K) pathway (Buss et al. 2009; Laplante et al. 2012). P70/ribosomal protein S6 kinase (S6K) and 4E-binding protein 1 (4E-BP1) are two main downstream targets of mTORC1. P70/S6K activation which is associated with enhanced protein synthesis can leads to cardiac hypertrophy (Boluyt et al. 1997; Di et al. 2012). Another downstream 4E-BP1 is an inhibitor of protein synthesis, which is inactivated by mTORC1. Phosphorylation of 4E-BP1 can accelerate the release of eukaryotic initiation factor 4E (eIF4E), allowing increased formation of the eIF4F translation factor complexes (Pham et al. 2000). Activation of this signaling pathway is not only involved in physiological hypertrophy but also taken part in pathological remodeling of the heart after MI, which can be improved by a mTORC1 inhibitor rapamycin (Buss et al. 2009; Di et al. 2012). However, it has been reported that rapamycin has some adverse effects such as body weight loss, increased risks of infection and cancer, and diabetes-like symptoms (Di et al. 2012; Chhajed et al. 2006; Weischer et al. 2007; Tataranni et al. 2011). Therefore, it is a clinical significance to screen a new drug inhibiting mTORC1 signaling with mild adverse effects.

Cardamonin (2,4-dihydroxy-6-methoxychalcone) is a naturally occurring chalcone mainly isolated from members of Zingiberaceae family (Hatziieremia et al. 2006). It possesses various pharmacological effects such as anti-platelet aggregation, anti-inflammatory activity, anti-nociceptive effect, anti-oxidative and vasorelaxant effects *in vivo* and *in vitro* (Hatziieremia et al. 2006; Shen et al. 2014; Li et al. 2015). Furthermore, more studies related to cardamonin are focused on chemopreventive properties in a variety of cancers such as breast, hematological, prostate and colorectal cancers, which are closely associated to inhibition of the mTORC1 signaling pathway (Tang et al. 2014; Niu et al. 2015, 2018; Shi et al. 2018). Our previous study has shown that cardamonin improves pressure overload-induced cardiac remodeling and dysfunction through inhibition of oxidative stress (Li et al. 2016). However, there are no reports about cardamonin's cardio-protective effects against ALVR in MI mice. Therefore, in the present study we wanted to establish whether cardamonin protected against ALVR through mTORC1 inhibition in mice with MI.

2. Investigations and results

2.1. Effects of cardamonin on heart weight/body weight ratio, body weight and cardiac function in MI mice

Among the three groups, the model group was not treated with cardamonin and the heart weight/body weight ratio in this group

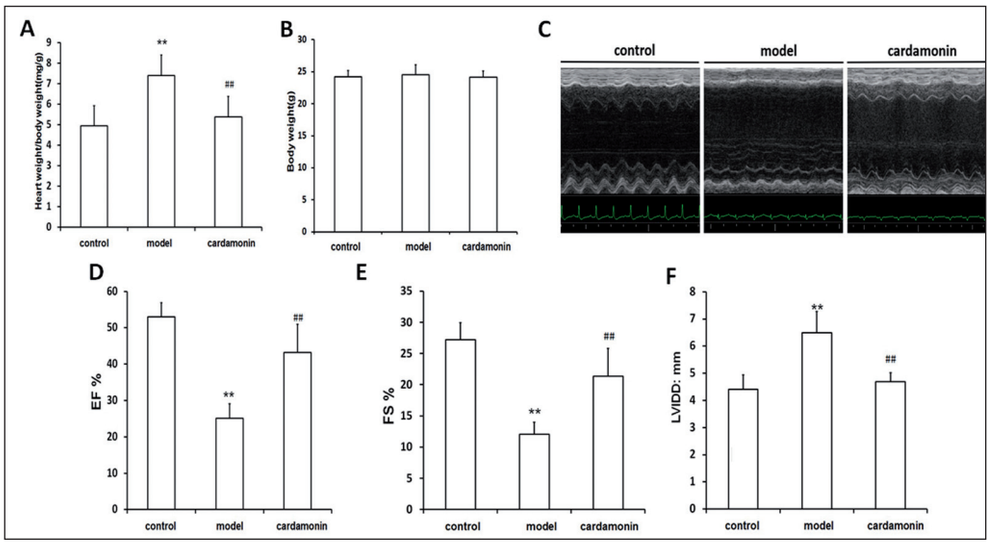

Fig. 1: Effects of cardamonin on heart weight/body weight ratio, body weight and cardiac function in MI mice. A, Ratio of heart weight to body weight (control: n=6; model: n=7; cardamonin: n=7). B, Body weight (control: n=6; model: n=7; cardamonin: n=7). C-F, Echocardiography measurement (control: n=6; model: n=7; cardamonin: n=7). MI, myocardial infarction; EF, ejection fraction; FS, fractional shortening; LVIDD, left ventricular internal diastolic diameter; control, mice after sham operation; model, mice with left descending coronary artery (LAD) ligation; cardamonin, mice with LAD ligation treated with cardamonin. Data are given as means±SEM. $^{**}P < 0.01$ vs control group, $^{\#\#}P < 0.01$ vs model group.

was the highest, indicating thet heart hypertrophy was provoked by MI (P<0.05). Treatment with cardamonin for two weeks significantly suppressed cardiac hypertrophy after MI, as indicated by the heart weight/body weight ratio (P<0.05) (Fig. 1A). However, there were no changes in body weight among the three groups (P>0.05) (Fig. 1B).

Two weeks after MI, heart systolic function was considerably impaired, as indicated by LVEF and LVFS measurements (P<0.05). Treatment with cardamonin greatly improved cardiac systolic function two weeks after MI (P<0.05) (Fig. 1C, D, E). An increase in LVIDD is an index for cardiac dilation. LVIDD was highest in model group, but was significantly smaller in the cardamonin group (P<0.05) (Fig. 1C, F).

Taken together, these results indicated that cardamonin alleviated heart hypertrophy and improved heart dysfunction after MI.

2.2. Effects of cardamonin on cardiac fibrotic area and cardiomyocyte hypertrophy in MI mice

After surgery-induced MI, the size of cardiomyocytes increased significantly in the left ventricle of vehicle-treated mice compared with sham mice (P<0.05). Two weeks after cardamonin treatment in MI mice, fibrotic area and cardiomyocyte size were declined notably compared to those of the model group (P<0.05), indicating that cardamonin decreased cardiac fibrosis and reduced cardiomyocyte size in MI mice (Fig. 2A, B, C, D).

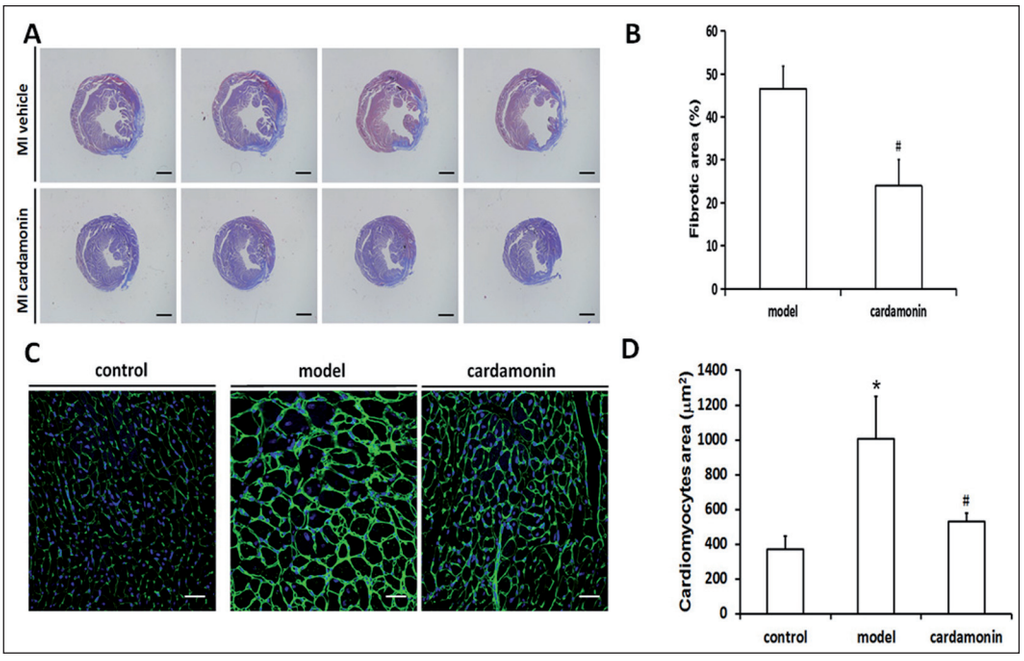

Fig. 2: Effects of cardamonin on cardiac fibrotic area and cardiomyocyte hypertrophy in MI mice. A, Masson's staining was used to display fibrotic areas (in blue). B, Quantitation of fibrotic area (model: n=3; cardamonin: n=3). C, Wheat germ agglutinin staining was used to display the size of cardiomyocytes. D, Quantitation of cross areas of cardiomyocytes (control: n=3; model: n=3; cardamonin: n=3). Data are given as means±SEM. $^{*}P < 0.05$ vs control group, $^{\#}P < 0.05$ vs model group.

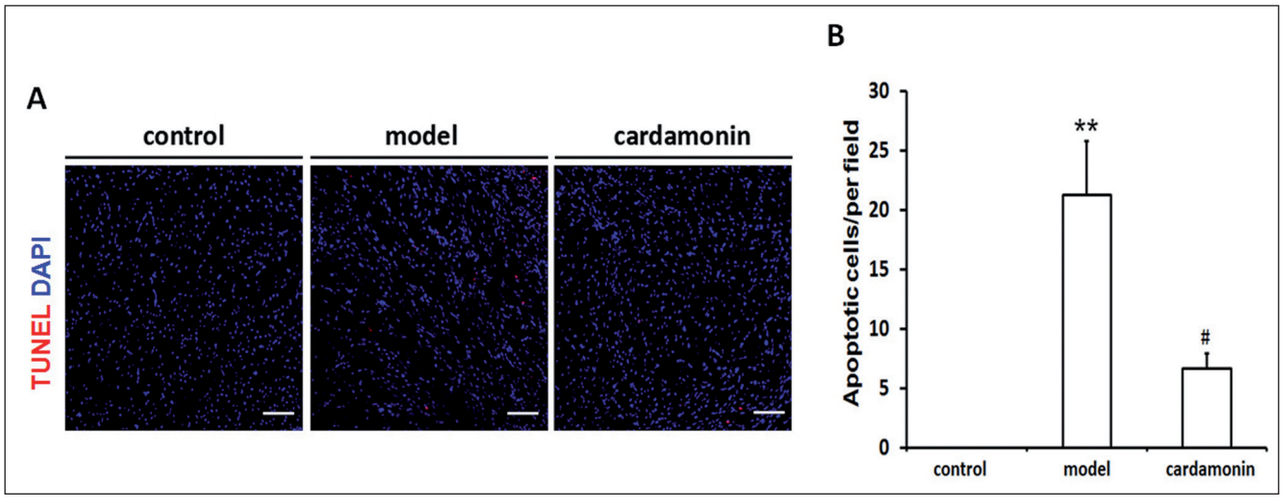

Fig. 3: Effect of cardamonin on cell apoptosis of border area in MI mice. A, TUNEL staining was used to show cell apoptosis of border area. B, Quantitation of apoptosis cell number (control: n=3; model: n=3; cardamonin: n=3). Data are given as means±SEM. $^{**}P < 0.01$ vs control group, $^{\#}P < 0.05$ vs model group.

2.3. Effects of cardamonin on cell apoptosis of border area in MI mice

Two weeks after MI, cell apoptosis of border area in MI mice increased notably as compared to mice with sham operation (P<0.01). After treatment with cardamonin, change in cell apoptosis were less in cardamonin-treated mice than in vehicle-treated MI mice (P<0.05). In total, the result showed that cardamonin can reduce cell apoptosis of border area in MI mice (Fig. 3A, B).

2.4. Effects of cardamonin on mTORC1 signaling in heart of MI mice and H9C2 cell line

To further investigate the possible molecular mechanism by which cardamonin improved cardiac remodeling, we examined the mTORC1 signaling pathway *in vivo* and *in vitro*. After MI for two weeks, the phosphorylation of 4E-BP1 Thr37/46 and S6 Ser235/236 in heart of MI mice were slightly increased as compared to mice of sham group (P>0.05). Cardamonin administration can significantly decrease the phosphorylation of 4E-BP1 Thr37/46 and S6 Ser235/236 in heart after mice with MI (P<0.05) (Fig. 4A, B). *In vitro*, treatment of H2C9 cells with cardamonin also significantly reduced 4E-BP1 and S6 phosphorylation (Fig. 4C, D).

The Co-IP assay was performed to test the assembly of mTORC1 complex. The mTOR-Raptor complex was disrupted by cardamonin in H9C2 cells (P<0.05) (Fig. 4E, F). Expressions of mTOR and Raptor were unchanged after cardamonin treatment (P>0.05) (Fig. 4E, F). In conclusion, cardamonin medication can inhibit mTORC1 signaling in heart of MI mice through disturbing mTOR-Raptor association.

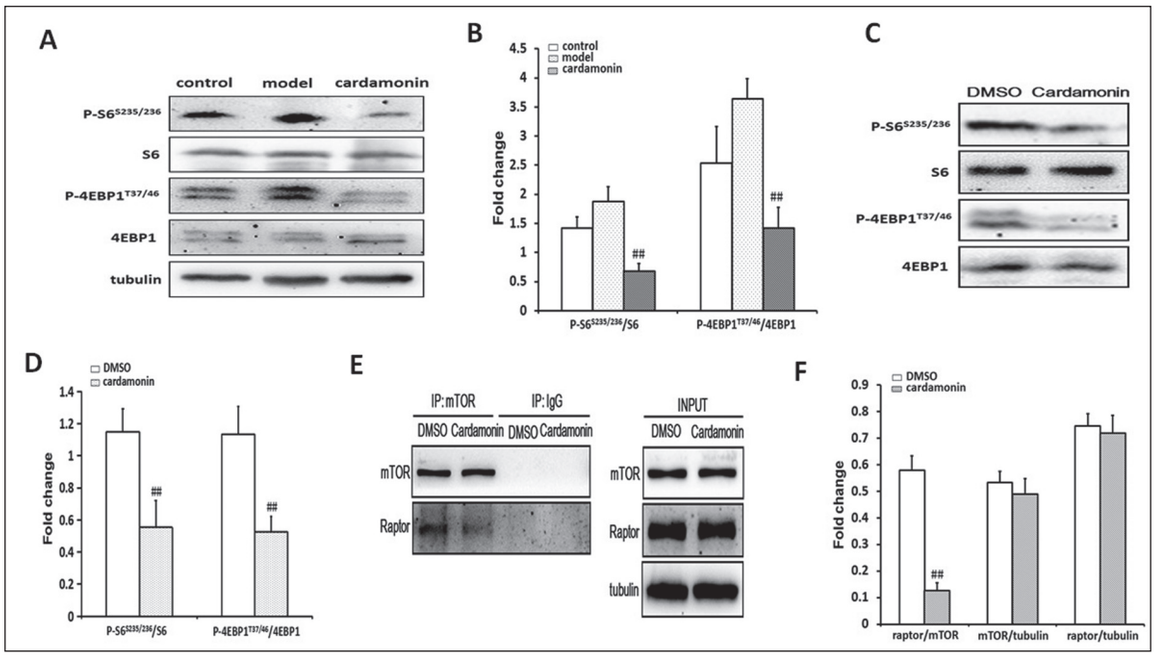

Fig. 4: Effects of cardamonin on mTORC1 signaling in heart of MI mice and H9C2 cell line. A, Western blot analysis of 4E-BP1 and S6 phosphorylation in heart tissues of MI mice. B, Quantitative study (control: n=3; model: n=3; cardamonin: n=3). C, Western blot analysis of 4E-BP1 and S6 phosphorylation in H9C2 cells. D, Quantitative study (DMSO: n=3; cardamonin: n=3). E, The Co-IP assay was performed to test the assembly of mTOR-Raptor complex. F, Quantitative study (DMSO: n=3; cardamonin: n=3). mTORC1, mechanistic target of rapamycin complex 1; 4E-BP1, 4E-binding protein 1; S6, ribosomal S6; mTOR, mechanistic target of rapamycin; Co-IP, co-immunoprecipitation. Data are given as means±SEM. $^{\#\#}P < 0.01$ vs model group or DMSO group.

3. Discussion

The main finding of this study was that targeting mTORC1 signaling pathway by cardamonin can prevent adverse left ventricular remodeling and limit infarct size in mice after MI, which was not reported elsewhere.

It is known that mTORC1 plays a significant role in regulating cellular growth and development (Laplante et al. 2012). Activated mTORC1 phosphorylates its downstream target S6K1 and 4E-BP1, and subsequently promotes mRNA transcription and protein translation. Studies show that the P70/S6K phosphorylates ribosomal S6 that predominates this function (Laplante et al. 2012; Di et al. 2012). Yu and his team has first reported that cardamonin may play a key role in reducing insulin resistance and smooth muscle proliferation of thoracic aorta in fructose-induced rats, possibly via a mechanism involving the inhibition of insulin/mTORC1 signaling as indicative of mTOR, P70S6K1 and 4E-BP1 mRNA downregulation (Liao et al. 2010). Deng and his colleges have documented that cardamonin inhibited proliferation and induced apoptosis of A549 cells through directly interacting with mTOR independently of binding with 12 kDa FK506 binding protein (FKBP12) (Tang et al. 2014). Furthermore, they go on reporting that cardamonin inhibited the invasion and metastasis of Lewis lung carcinoma cells through inhibiting mTOR phosphorylation and mTOR protein expression was not changed after cardamonin treatment (Niu et al. 2015). The regulatory-associated protein of TOR (Raptor) is a major component of mTORC1. It has been indicated that Raptor mainly mediated the inhibition of cardamonin on mTORC1 in ovarian cancer SKOV3 cells and the phosphorylation and protein expression of Raptor were significantly suppressed by cardamonin (Shi et al. 2018). In our study, we found that cardamonin therapy can inhibit mTORC1 signaling in heart of MI mice and H9C2 cells as indicative of the down-regulated phosphorylation of 4E-BP1 and S6. Therefore, we can conclude that cardamonin has a property of mTORC1 inhibition.

mTORC1 consists of Raptor, mammalian lethal with Sec13 protein 8 (mLST8), and the two inhibitory subunits proline-rich Akt substrate of 40 kDa (PRAS40) and DEP domain containing mTOR-interacting protein (DEPTOR) (Rabanal-Ruiz et al. 2018). Among these elements, Raptor and Deptor positively and negatively regulate mTOR activation, respectively (Rabanal-Ruiz et al. 2018). It is reported that disruption the assembling of mTOR-Raptor association can cause de-phosphorylation of S6K1 and 4E-BP1 (Li et al. 2018). In the study, we found that cardamonin can disrupt mTOR-Raptor relation in H9C2 cells, indicating mTORC1 inhibition of cardamonin was closely associated with mTOR-Raptor complex dissociation. Although cardamonin is reported to regress mTOR mRNA expression or Raptor protein express in different cell lines (Niu et al. 2015; Liao et al. 2010), in our study protein expressions of mTOR and Raptor were unchanged after treatment with cardamonin in H9C2 cell line.

Rapamycin and its derivatives are artificial inhibitors against the mTORC1 signaling pathway. It has been documented that rapamycin and everolimus, mTORC1 inhibitors, can limit infarct size and attenuate ALVR after MI (Buss et al. 2009; Di et al. 2012). However, their severe adverse effects limit the clinical application and prompt the search for better substitutes (Di et al. 2012; Chhajed et al. 2006; Weischer et al. 2007; Tataranni et al. 2011). Cardamonin is found in conventional Chinese medicines in high concentration, such as *Alpinia katsumadai* and *Amomum subulatum* (Shen et al. 2014; Li et al. 2015). Our previous study has shown that pressure overload can induce severe oxidative stress, and that cardamonin medication acts cardio-protective by blocking excessive oxidative stress and apoptosis through mitochondria-dependent pathways (Li et al. 2016). In the present study, due to mTORC1 inhibition of cardamonin reported in the literature, we went on studying cardamonin mediated cardio-protection in MI mice. After treatment with cardamonin for two weeks, heart hypertrophy and heart dysfunction were alleviated, and cardiac fibrosis, cardiomyocyte size and cell apoptosis of border area were decreased, indicating that cardamonin can render cardio-protection against ALVR in mice with MI.

In conclusion, cardamonin can exert cardio-protective effects against ALVR including cardiomyocyte hypertrophy, myocardial fibrosis and cell apoptosis in MI mice through its mTORC1 inhibition, which is closely associated with mTOR-Raptor complex dissociation.

4. Experimental

4.1. Mice, MI model and medication

Eight-week-old male mice from C57BL/6 background were housed in groups with 12 h dark-light cycles and free access to food and water. These conditions are in accordance with the Guide for the Care and Use of Laboratory Animals published by the US National Institutes of Health (NIH publication no. 85-23, revised in 1996), and the regulations on mouse welfare and ethics of Nanjing University.

MI was generated following a method previously reported in mice with slight modifications (Matsumoto et al. 2011). Briefly, mice were anaesthetized intraperitoneally with pentobarbital sodium (30-50 mg/kg). A 20-gauge polyethylene catheter was intubated into the trachea and a volume-cycled rodent respirator (model 683; Harvard Apparatus, Holliston, MA) provided positive pressure ventilation at 2-3 ml/cycle and a respiratory rate of 120 cycles/min. After the thoracic cavity at the level of the fourth rib and along the left sternal border was opened, left anterior descending coronary artery (LAD) was ligated with a 7-0 silk suture 3 mm from the tip of the left auricle. The chest wall was closed with a continuous 6-0 prolene suture, followed by a 4-0 polyester suture to close the skin. The procedure of sham operation was the same as the above-mentioned MI induction without LAD ligation.

Cardamonin (purity 98 %, Cas No. 19309-14-9, Nanjing DASF Bio-Technology Co., Ltd., Nanjing, china) was dissolved into phosphate buffer solution (PBS). Twenty mice were randomly assigned into three groups as follows: sham group (without LAD occlusion and only received an intraperitoneal injection of 10 ml/kg/day PBS, n=6), model group (LAD ligation and received an intraperitoneal injection of 10 ml/kg/day PBS, n=7) and cardamonin-treated group (LAD ligation and received an intraperitoneal injection gavage of cardamonin at the dose of 20 mg/kg/day, n=7). Furthermore, all groups were administered accordingly for 2 weeks.

4.2. Cardiac function assessment by echocardiography

An echocardiographic examination was performed on day 14 following the MI induction using a Vevo 770 UBM system (Visual Sonics, Toronto, Canada), equipped with a 30-MHz transducer, was used for noninvasive transthoracic echocardiography. Two-dimensional guided M-mode tracings were recorded. The internal diameter of the LV in the short-axis plane was measured at end diastole and end systole from M-mode recordings just below the tips of the mitral valve leaflets. After measurement, LV internal diameter at end-diastole (LVIDD) as indicative of cardiac diastolic function were measured. Two indexes of cardiac systolic function including LV fractional shortening (LVFS) and LV ejection fraction (LVEF) were calculated.

4.3. Western blot analysis

Western blot analyses were performed as reported previously (Di et al. 2012). Heart tissues of mice were dissected and snap-frozen in liquid nitrogen until use. Tissue lysates of mice were prepared in lysis buffer (20 mM Tris, 150 mM NaCl, 10% glycerol, 20 mM glycerophosphate, 1% NP40, 5 mM EDTA, 0.5 mM EGTA, 1 mM Na3VO4, 0.5 mM PMSF, 1 mM benzamidine, 1 mM DTT, 50 mM NaF, 4 μM leupeptin, pH = 8.0). Proteins were resolved by 10% SDS-PAGE and transferred to PVDF membranes (Millipore, Billerica, MA, USA). Membranes were blocked with 5% non-fat milk in TBST (50 mM Tris, 150 mM NaCl, 0.5 mM Tween-20, pH = 7.5) and then incubated overnight with primary antibodies. The following antibodies were purchased from Cell Signaling Technology Inc. (Danvers, MA): S6, phosphor-S6 (S235/236), 4E-BP1, phosphor-4E-BP1 (T37/46), mTOR, Raptor. Tubulin and HRP-linked secondary antibodies were purchased from BD bioscience (Bedford, MA, USA) and Thermos Scientific (Pittsburgh, PA, USA), respectively. Image J software (NIH) was used to perform densitometric analysis.

4.4. Cell culture and co-immunoprecipitation (Co-IP)

H9C2 cells were grown at 37 °C in Dulbecco's modified Eagle's medium supplemented with 10% fetal calf serum. These cells were treated with cardamonin (20 μM) every 24 h or dimethyl sulfoxide (DMSO) and were collected after 48 h for Western blot analysis. For Co-IP experiment, primary anti-mTOR antibody or Ig G were added to cell lysates and incubated with gentle rocking overnight at 4 °C. After addition of 30 μl of 50% slurry of the protein A agarose, the incubation was continued for 3 h with gentle rotation. Immunoprecipitates were washed three times with ice-cold PBS/1× lysis buffer. Immunoprecipitated proteins were detected by Western blot using 8% SDS-PAGE as described (Di et al. 2012).

4.5. Histology and immunofluorescence staining

The protocols of Masson's staining and immunofluorescence (IF) were performed as described previously (Aytekin et al. 2014). Briefly, heart samples were first washed with ice-cold PBS and then fixed in 4 % paraformaldehyde at 4 °C. The samples were processed successively by (a) a 30 min washing in PBS at 4 °C; (b) 15 min each in 30 %, 50 %, 75 %, and 85 % ethanol, and then 2 × 10 min of incubation in 95 and 100 % ethanol at room temperature (RT); (c) 3 × 10 min of incubation in xylene at RT; (d) 20 min of incubation in paraffin/xylene (1:1) at 65 °C; (e) 3 × 30 min of incubation

in fresh paraffin at 65 °C. The processed samples were embedded in paraffin and sectioned into 6 µm thick, and then the sections were stained.
IF staining was performed using anti-wheat germ agglutinin (WGA) (Abcam) antibody at 4 °C overnight. Fluorescence microscopy images were obtained with a Research Fluorescence Microscope (Olympus America Inc., Center Valley, PA) equipped with a digital camera. Images were collected and recorded by using Adobe Photoshop® 5.0 (Adobe Systems Inc., San Jose, CA) on an IBM R52 computer (IBM, Armonk, NY). Area of cardiomyocytes were measured with 400× magnification, and averaged after determining in 5 high-power fields.

4.6. Terminal deoxynucleotidyl transferase-mediated dUTP nick end labeling (TUNEL) assay

TUNEL assay was performed as previously reported (Popper et al. 1997). Briefly, the sections were treated with 20 mg/mL of proteinase K and were incubated with terminal deoxynucleotidyl transferase and biotinylated deoxyuridine triphosphate.

4.7. Statistical analysis

Data are presented as mean±SEM values. For comparisons between two groups, statistical significance was determined using one-way ANOVA followed by Tukey's post-hoc test. A $P < 0.05$ was considered statistically significant.

Acknowledgements: This work was supported by the National Natural Science Foundation of China (grant number 81600296).

Conflict of interest : None declared.

References

Aytekin M, Tonelli AR, Farver CF, Feldstein AE, Dweik RA (2014) Leptin deficiency recapitulates the histological features of pulmonary arterial hypertension in mice. Int J Clin Exp Pathol 7: 1935-1946.

Benjamin EJ, Blaha MJ, Chiuve SE, Cushman M, Das SR, Deo R, de Ferranti SD, Floyd J, Fornage M, Gillespie C, Isasi CR, Jimenez MC, Jordan LC, Judd SE, Lackland D, Lichtman JH, Lisabeth L, Liu S, Longenecker CT, Mackey RH, Matsushita K, Mozaffarian D, Mussolino ME, Nasir K, Neumar RW, Palaniappan L, Pandey DK, Thiagarajan RR, Reeves MJ, Ritchey M, Rodriguez CJ, Roth GA, Rosamond WD, Sasson C, Towfighi A, Tsao CW, Turner MB, Virani SS, Voeks JH, Willey JZ, Wilkins JT, Wu JH, Alger HM, Wong SS, Muntner P (2017) Heart Disease and Stroke Statistics-2017 Update: A Report from the American Heart Association. Circulation 135: e146-603.

Buss SJ, Muenz S, Riffel JH, Malekar P, Hagenmueller M, Weiss CS, Bea F, Bekeredjian R, Schinke-Braun M, Izumo S, Katus HA, Hardt SE (2009) Beneficial effects of mammalian target of rapamycin inhibition on left ventricular remodeling after myocardial infarction. J Am Coll Cardiol 54: 2435-2446.

Boluyt MO, Zheng JS, Younes A, Long X, O'Neill L, Silverman H, Lakatta EG, Crow MT (1997) Rapamycin inhibits alpha 1-adrenergic receptor-stimulated cardiac myocyte hypertrophy but not activation of hypertrophy-associated genes. Evidence for involvement of P70 S6 kinase. Circ Res 81:176-186.

Chhajed PN, Dickenmann M, Bubendorf L, Mayr M, Steiger J, Tamm M (2006) Patterns of pulmonary complications associated with sirolimus. Respiration 73:367-374.

Cohn JN, Ferrari R, Sharpe N (2000) Cardiac remodeling – concepts and clinical implications: a consensus paper from an international forum on cardiac remodeling. J Am Coll Cardiol 35: 569-582.

Di R, Wu X, Chang Z, Zhao X, Feng Q, Lu S, Luan Q, Hemmings BA, Li X, Yang Z (2012) S6k inhibition renders cardiac protection against myocardial infarction through Pdk1 phosphorylation of Akt. Biochem J 441: 199-207.

Hatziieremia S, Gray AI, Ferro VA, Paul A, Plevin R (2006) The effects of cardamonin on lipopolysaccharide-induced inflammatory protein production and Map kinase and Nfkappab signalling pathways in monocytes/macrophages. Br J Pharmacol 149:188-198.

Laplante M, Sabatini DM (2012) Mtor signaling in growth control and disease. Cell 149: 274-293.

Li YY, Huang SS, Lee MM, Deng JS, Huang GJ (2015) Anti-inflammatory activities of cardamonin from Alpinia katsumadai through heme oxygenase-1 induction and inhibition of Nf-Kappab and Mapk signaling pathway in the carrageenan-induced paw edema. Int Immunopharmacol 25: 332-339.

Li W, Wu X, Li M, Wang Z, Li B, Qu X, Chen S (2016) Cardamonin alleviates pressure overload-induced cardiac remodeling and dysfunction through inhibition of oxidative dtress. J Cardiovasc Pharmacol 68: 441-445.

Li X, Li Z, Song Y, Liu W, Liu Z (2018) The Mtor kinase inhibitor Cz415 inhibits human papillary thyroid carcinoma cell growth. Cell Physiol Biochem 46: 579-590.

Liao Q, Shi DH, Zheng W, Xu XJ, Yu YH (2010) Antiproliferation of cardamonin is involved in Mtor on aortic smooth muscle cells in high fructose-induced insulin resistance rats. Eur J Pharmacol 641:179-186.

Matsumoto K, Ogawa M, Suzuki J, Hirata Y, Nagai R, Isobe M (2011) Regulatory T lymphocytes attenuate myocardial infarction-induced ventricular remodeling in mice. Int Heart J 52: 382-587.

Niu PG, Zhang YX, Shi DH, Liu Y, Chen YY, Deng J (2015) Cardamonin inhibits metastasis of Lewis lung carcinoma cells by decreasing Mtor activity. PLoS One 10:e0127778.

Niu P, Shi D, Zhang S, Zhu Y, Zhou J (2018) Cardamonin enhances the anti-proliferative effect of cisplatin on ovarian cancer. Oncol Lett 15: 3991-3997.

Pham FH, Sugden PH, Clerk A (2000) Regulation of protein kinase B and 4e-Bp1 by oxidative stress in cardiac myocytes. Circ Res 86:1252-1258.

Popper P, Farber DB, Micevych PE, Minoofar K, Bronstein JM (1997) Trpm-2 expression and tunel ataining in neurodegenerative diseases: studies in Wobbler and Rd mice. Exp Neurol 143: 246-254.

Rabanal-Ruiz Y, Korolchuk VI (2018) Mtorc1 and nutrient homeostasis: the central Role of the lysosome. Int J Mol Sci 19: pii: E818.

Shen YJ, Zhu XX, Yang X, Jin B, Lu JJ, Ding B, Ding ZS, Chen SH (2014). Cardamonin inhibits angiotensin Ii-induced vascular smooth muscle cell proliferation and migration by downregulating P38 Mapk, Akt, and Erk phosphorylation. J Nat Med 68: 623-629.

Shi D, Zhu Y, Niu P, Zhou J, Chen H (2018) Raptor mediates the antiproliferation of cardamonin by Mtorc1 inhibition in Skov3 cells. Onco Targets Ther 11: 757-767.

Tang Y, Fang Q, Shi D, Niu P, Chen Y, Deng J (2014) Mtor inhibition of cardamonin on antiproliferation of A549 cells is involved in a Fkbp12 independent fashion. Life Sci 99: 44-51.

Tataranni T, Biondi G, Cariello M, Mangino M, Colucci G, Rutigliano M, Ditonno P, Schena FP, Gesualdo L, Grandaliano G (2011) Rapamycin-induced hypophosphatemia and insulin resistance are associated with Mtorc2 activation and Klotho expression. Am J Transplant 11: 1656-1664.

Weischer M, Rocken M, Berneburg M (2007) Calcineurin inhibitors and rapamycin: cancer protection or promotion? Exp Dermatol 16: 385-393.

Zaman AG, Helft G, Worthley SG, Badimon JJ (2000) The role of plaque rupture and thrombosis in coronary artery disease. Atherosclerosis 149: 251-266.